aptara	JCE	jce959	Dispatch: August 24, 2007	CE: AN
	Journal	MSP No.	No. of pages: 7	PE: Ryan

The Role of Cardiac Tissue Alignment in Modulating Electrical Function

CHIUNG-YIN CHUNG, M.S.,* HAROLD BIEN, M.S.,* and EMILIA ENTCHEVA, PH.D.*,†

From the *Department of Biomedical Engineering, and †Department of Biophysics and Physiology, SUNY Stony Brook, Stony Brook, New York, USA

Cardiac Tissue Alignment and Function. ***Introduction:*** **Most cardiac arrhythmias are associated with pathology-triggered ion channel remodeling. However, multicellular effects, for example, exaggerated anisotropy and altered cell-to-cell coupling, can also indirectly affect action potential morphology and electrical stability via changed electrotonus. These changes are particularly relevant in structural heart disease, including hypertrophy and infarction. Recent computational studies showed that electrotonus factors into stability by altering dynamic properties (restitution). We experimentally address the question of how cell alignment and connectivity alter tissue function and whether these effects depend on direction of wave propagation.**

Methods and Results: **We show that cardiac cell arrangement can alter electrical stability in an *in vitro* cardiac tissue model by mechanisms both dependent and independent of the direction of wave propagation, and local structural remodeling can be felt beyond a space constant. Notably, restitution of action potential duration (APD) and conduction velocity was significantly steepened in the direction of cell alignment. Furthermore, prolongation of APD and calcium transient duration was found in highly anisotropic cell networks, both for longitudinal and transverse propagation. This is in contrast to expected correlation between wave propagation direction and APD based on electrotonic effects only, but is consistent with our findings of increased cell size and secretion of atrial natriuretic factor, a hypertrophy marker, in the aligned structures.**

Conclusion: **Our results show that anisotropic structure is a potent modulator of electrical stability via electrotonus and molecular signaling. Tissue alignment must be taken into account in experimental and computational models of arrhythmia generation and in designing effective treatment therapies.** *(J Cardiovasc Electrophysiol, Vol. pp. 1-7)*

arrhythmia, mechanisms, calcium, cellular, cell culture, membrane potential, myocytes

Introduction

The heart is an anatomically and functionally anisotropic organ, with properties dependent on the underlying structure—propagation of electrical signals along the alignment of muscle fibers is faster than transverse to fiber alignment. During diseased states, structural remodeling altering the anisotropy has a major impact on electrophysiological function. Development of electrical instabilities and arrhythmias are serious potential consequences. Such structural changes are seen in myocardial infarct (MI) where surviving tissue has loss of side-to-side connections between muscle fibers and "stringy" fibrosis encroaching on border zone myocytes causes heterogeneity in orientation.[1-4] Noninfarcted myocytes undergo hypertrophic growth in order to sustain cardiac output. In cardiac hypertrophy itself, exaggerated anisotropy is often seen due to reduced coupling between fibers and additional fibrosis and collagen deposition.[3,5]

Structural changes are paralleled by electrophysiological remodeling that leads to increased susceptibility to arrhythmias. For example, in hypertrophy due to either compensation in MI or pressure overload, a major arrhythmogenic change is action potential duration (APD) prolongation caused mainly by decreased potassium channel (Ito) function and protein expression.[6-8] Longer APD leads to more frequent wavefront–waveback collisions potentially resulting in conduction block and reentry.[9] Hypertrophy-associated APD prolongation can be caused also by calcium channel remodeling. However, changes in the current are dependent on the stage of hypertrophy; mild hypertrophy sees an increase in ICaL, while severe hypertrophy and heart failure result in decreased ICaL.[10]

Cell-level electrical remodeling can be further exacerbated by changes in cell arrangement. The anisotropic structure of cardiac tissue determined by the oriented and elongated cell morphology and cell-to-cell connections (gap junctions) establishes different electrotonic loading in propagation longitudinal or transverse to fiber orientation and produces well-known functional anisotropy. Due to greater proportion of highly conducting cytoplasm and greater number of gap junctions, overall resistance is less and electrotonic

This study was funded by grants from the Whitaker Foundation (RG-02-0654), The American Heart Association (0430307N), and the National Science Foundation (BES-0503336).

Chiun-Yin Chung received financial support from Stony Brook University for presentation of the material (in part) at the BMES 2005 Conference.

This study was presented in part at the Heart Rhythm Society's 28th Annual Scientific Sessions, Denver May 2007 and published in abstract form.

Address for correspondence: Dr. Emilia Entcheva, Ph.D., Department of Biomedical Engineering, Stony Brook University, HSC T18-030, Stony Brook, NY 11794-8181. Fax: 631-444-6646; E-mail: emilia.entcheva@sunysb.edu

Received 26 January 2006; Revised manuscript received 3 July 2007; Accepted for publication 9 July 2007.

doi: 10.1111/j.1540-8167.2007.00959.x

load is greater in the longitudinal direction; thus, propagation proceeds faster.[11,12] Larger electrotonus in longitudinal propagation also translates into a flattened maximum upstroke rate of depolarization.[13] This functional anisotropy may be affected in diseased states where structural anisotropy may be exaggerated, leading to greater heterogeneity and potential for arrhythmia development.

The arrhythmogenicity of cardiac tissue is also affected by its dynamic response to frequency. The frequency response (restitution) of cardiac tissue traditionally describes a correlation between the diastolic interval and the subsequent action potential. It has been proposed that a steeper APD restitution slope may indicate a more unstable system with increased susceptibility to the development of alternans, a precursor to deadly fibrillation. Studies have demonstrated that APD restitution, modulated by restitution of conduction velocity, plays a critical role in break up of stable spirals into fibrillation.[14–18] The structure and the dynamics of cardiac tissue have mostly been treated as separate factors in determining the arrhythmogenic state. Recent theoretical studies have shown a potential interaction between restitution and electrotonus thus questioning the true independence of these two determinants of electrical stability.[17,18] Little experimental data exist addressing these interactions.

In this study, we sought to determine and isolate the effects of structure on electrophysiological function and stability in cardiac tissue. Specifically, we asked the following questions: (1) Is the frequency response (restitution) of aligned tissue dependent on the tissue structure? (2) Do structural features affect function remotely (outside of a space constant)? To address these questions, anisotropic neonatal rat cardiac myocyte networks were grown using topographic guidance on 3D polydimethylsiloxane (PDMS) surfaces. The dynamic response of these networks was probed over a range of stimulation frequencies in the voltage and calcium domains.

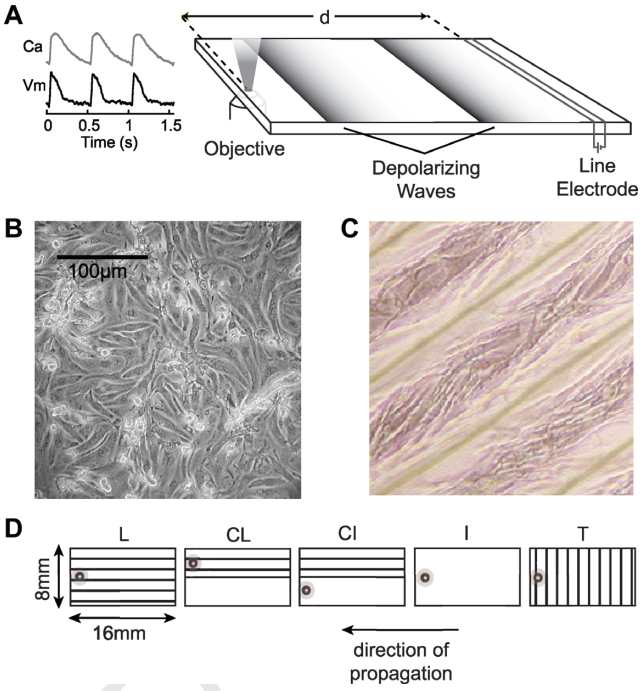

COLOUR FIG.

Figure 1. *Functional measurement setup. (A) Cells plated on PDMS scaffolds were stimulated (10 V/m) at one end with a line electrode. Propagated signals were collected with a PMT at the opposite end (example calcium and voltage signals shown). Distance (d) between the electrode and objective was used in conduction velocity calculations along with the lag time between stimulus and observed signal. (B) Cardiac myocytes grown on flat surfaces showed random orientation. (C) Myocytes grown on grooved surfaces showed anisotropic growth aligned with the grooves. (D) Five experimental groups were used: longitudinal (L) with grooves parallel to the direction of propagation; transverse (T) with grooves perpendicular to the direction of propagation; control isotropic (I); and combination samples with both grooved (CL) and isotropic (CI) regions, each region probed separately more than a space constant away from the border. Location of signal acquisition in experimental group is indicated on each scaffold.*

Methods

Primary Myocyte Culture and Anisotropic Growth

Neonatal rat cardiac myocytes were isolated and plated as previously described.[19] Briefly, myocytes from 3-day-old neonatal Sprague–Dawley rats were isolated by enzymatic digestion overnight with trypsin (1 mg/mL, 4°C, USB, Cleveland, OH, USA), then collagenase (1 mg/mL, 37°C, Worthington, Lakewood, NJ, USA). After 90 minutes preplating to remove the fibroblast population, myocytes were plated at high density (4×10^5 cells/cm^2) onto fibronectin-coated polydimethylsiloxane (PDMS, Sylgard 184, Dow Corning, Midland, MI, USA) scaffolds with varying topographical features produced by molding onto metal templates fabricated by acoustic micromachining.[19,20] Flat, uniformly grooved, and combination (combined flat and grooved) scaffolds (Fig. 1B–D) were used in this study.

Dynamic Functional Measurements

Across five cultures, on days 5 to 7 after cell plating, myocytes were washed and equilibrated at room temperature in Tyrode's solution (1.33 mM Ca^{2+}, 5 mM glucose, 5 mM HEPES, 1 mM $MgCl_2$, 5.4 mM KCl, 135 mM NaCl, 0.33 mM NaH_2PO_4, pH 7.4) and costained for transmembrane voltage and intracellular calcium with di-8 ANEPPS and fura-2 AM (Molecular Probes, Eugene, OR, USA), respectively. Stained myocytes were transferred to a temperature-controlled (~30°C) experimental chamber perfused with fresh Tyrode's solution. In the experimental chamber, cells were stimulated with a Pt line electrode at one end of the scaffold, initiating a planar wave. Cells were paced at several frequencies following a dynamic restitution protocol.[16] Frequency was varied from 1 Hz to 2 Hz in 0.5 Hz steps and thereafter in 0.2 Hz increments. Fluorescence signals were recorded with a photomultiplier tube at a fixed distance (1.2–1.6 cm) from the electrode (Fig. 1A) at a sampling rate of 1,000 Hz. After achieving steady state by pacing for 60 beats,[21] 20 transients in the voltage and then the calcium domain were collected. Cells were paced until they failed to follow 1:1 (occurrence of alternans or conduction block). As shown in Figure 1D, five experimental groups with varying anisotropic structure were used: surfaces with grooves aligned longitudinal (L) to propagation, n = 12, surfaces with grooves aligned transversely (T) to propagation, n = 11, flat isotropic controls (I), n = 9, and combination scaffolds with both isotropic (CI), n = 10, and grooved (CL), n = 15, features, each configuration probed individually at least 500 μm away from the anisotropic/isotropic border (Fig. 1D).

Data Processing and Analysis

Collected fluorescence signals were temporally filtered using a polynomial filter (Savitsky-Golay) of second order and analyzed with a custom-made Matlab (Mathworks, Natick, MA, USA) program. Conduction velocity (CV) was estimated from the straight line distance, d, between the stimulating electrode and the acquisition site and the lag time between stimulation pulse and acquired response (Fig. 1A). This is a conservative measure of CV; effective velocity along the straight line path may be lower than the actual velocity if conduction occurs along a curved path. Aside from CV, functional parameters of interest were action potential duration at 80% repolarization (APD), calcium transient duration at 80% return (CTD), and estimated wavelength of propagation (W). The restitution behavior was characterized by linear fits to the frequency response of individual samples and determining average linear slope using Excel (Microsoft, Redmond, WA, USA). Statistical significance was determined with multiway analysis of variance (ANOVA) in Matlab with $P < 0.01$ considered significant, followed by Tukey post hoc testing.

Macroscopic Optical Mapping and Analysis

Macroscopic spatial mapping of fluorescent signals in combination samples was done 5 days after plating using an intensified CMOS camera system with 1,280 × 1,024 pixel resolution, as previously described.[22] The cells were stained with a calcium-sensitive dye, fluo-4 AM (Molecular Probes), excited at 488 nm through fiber optic light guides. Fluorescent movies of wave propagation in the tissue at 30°C were collected at several frequencies after arrival at steady state at a frame rate of 200 frames per second and a sensor-determined spatial resolution of 22 μm.

For propagation maps, raw data were binned (10 × 10) and analyzed in customized Matlab software after filtering both spatially (Gaussian, 3-pixel kernel) and temporally (Savitsky-Golay, order 2, width 5) and cropping to a center region of interest spanning the anisotropic/isotropic border zone. Activation times for each pixel were calculated as 50% of the peak height in the upstroke. An isochrone map was interpolated at every 400 μm. Spatial profiles of CV during planar propagation were constructed. Average CV profiles were calculated by averaging CV of three consecutive transients at each pixel and across all pixels with the same distance from the anisotropic/isotropic border ($n = 7$).

Quantification of Hypertrophic Growth

Confocal images of connexin 43 (Cx43) and actin were taken at 60× to reveal cell structure. The high magnification resulted in a small field of view, but allowed proper cell area calculation. Quantification of cell size was done by manual outlining of cells ($n = 22$ for anisotropic, $n = 29$ for isotropic) in the images and automated analysis in Matlab. In addition, secreted atrial natriuretic factor (ANF) was quantified as a marker of hypertrophic growth[23] 24 hours post-culture medium change on anisotropic ($n = 10$) and isotropic ($n = 11$) networks 10 days after plating, using an ANF ELISA kit (Peninsula Laboratories, San Carlos, CA, USA). Statistical significance ($P < 0.01$) was determined using a paired *t*-test.

Results

In this study, a remarkable difference, induced by the anisotropic structure, was seen in action potential and calcium transient morphology (Fig. 2A, B). Results at single pacing frequencies had similar trends as the frequency-averaged graphs throughout most pacing frequencies. At both low (1 Hz) and high (3 Hz) frequencies, action potentials (Fig. 2A) were prolonged in L and T, compared with I controls (80% repolarization at dashed lines). Similarly, calcium transients (Fig. 2B) showed lengthened CTD at low pacing frequency (1 Hz). Thus, anisotropic structure resulted in slower recovery of systolic calcium levels and altered the repolarization phase of the AP. In addition, the mere presence of partial anisotropic structure in combination structures increased the APD, compared with I controls, so that APDL ≈ APDT > APDCL ≈ APDCI > APDI. Convergence of values was seen in APD and CTD at pacing frequencies greater than 3.5 Hz. Overall, structures with aligned tissue had prolonged APD ($P < 0.01$, Fig. 2C), with a parallel increase of CTD (Fig. 2D) at lower pacing frequencies.

A clear dependence of restitution properties on direction of propagation was observed in aligned structures. Propagation in L was found to be the most sensitive to frequency ($P < 0.01$), as assessed by average linear slope of the frequency response, in CV, APD, CTD, and wavelength (Fig. 3). Conversely, mere presence of an isotropic region

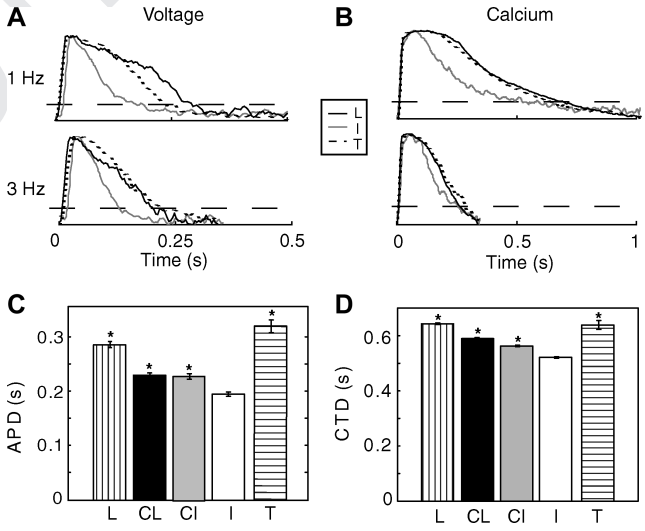

Figure 2. *APD and CTD prolongation seen in anisotropic tissue regardless of propagation direction. A and B. Example AP (left) and calcium transient (right) at low (1 Hz) and high (3 Hz) frequencies showed anisotropy-induced changes in APD and CTD with little modulatory effect of propagation direction. Comparison between low and high frequency pacing showed a greater change in APD at 80% repolarization (dashed line) in L than other configurations. Interestingly, mere presence of anisotropic structure had slower recovery of systolic calcium levels and altered repolarization phase. Black solid traces are L, gray solid traces are I, and black dashed traces are T. C. APD at 80% return at 1 Hz pacing frequency showed significantly longer ($P < 0.01$) APD in purely anisotropic samples (L and T) regardless of direction of propagation compared to I. APD in the combination samples with part anisotropic regions were intermediate between anisotropic and isotropic samples. Asterisks indicate significant difference from I ($P < 0.01$). D. Similar to APD, average CTD at 80% return at 1 Hz pacing frequency showed negligible effects from neighboring regions and little dependence on direction of propagation. L was significantly longer than I ($P < 0.01$).*

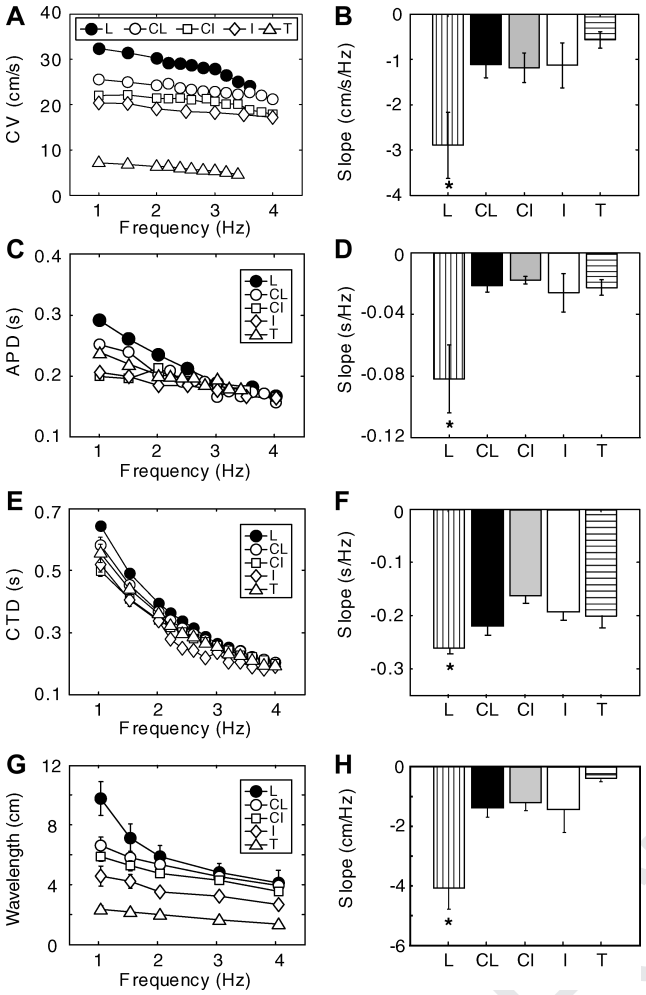

Figure 3. *Restitution is dependent on direction of propagation. The slope of the linear approximation of the frequency response was used to characterize restitution. The frequency response in L of CV (A), APD (C), CTD (E), and wavelength (G) showed a significantly steeper slope, while other samples had flatter responses (right). Asterisks indicate significant difference from I (P < 0.01).*

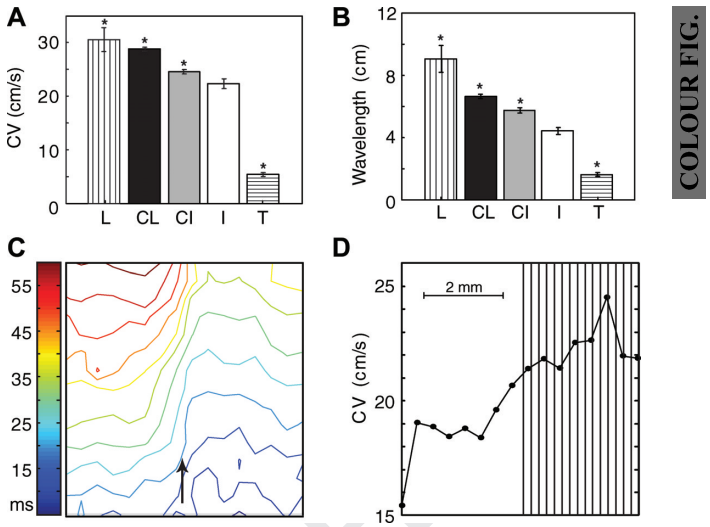

Figure 4. *Gradient CV and wavelength show potential remote effects of cell alignment and wavefront curvature. (A) Conduction velocity (CV) at 1 Hz pacing frequency changed with direction of propagation, as expected, but also in a dose-like manner by presence of neighboring regions of different alignment, as seen in combination samples (CL and CI). CV in L, CL, CI, and T were all significantly different than I (P < 0.01). (B) Wavelength calculated from the product of CV and APD also showed a significant dose-like effect from neighboring regions as well as directional differences, similar to CV. All samples were significantly different from I controls (P < 0.01), however the combination samples were not significantly different from each other. (C) Example isochrone map of calcium wave propagation in combination samples showed faster propagation in the anisotropic portion compared to the isotropic portion with concave curvature in the isotropic region and convex curvature in the anisotropic region. Propagation direction is shown by the arrow. (D) Activation maps matched average CV profiles (n = 7) that displayed a monotonic trend from the isotropic portion (left side of figure) to the anisotropic portion (right side of figure).*

(in combination samples) flattened the restitution, especially noticeable in the CV, APD, and wavelength frequency response.

In accord with previous studies, we saw that CV was highly dependent on the direction of propagation—fastest conduction longitudinal to the direction of tissue alignment and slowest in the transverse direction. Isotropic controls had intermediate CV (CVL > CVI > CVT), all significantly different from each other (P < 0.01, Fig. 4A) at 1 Hz pacing, a result matched in wavelength (Fig. 4B). At higher pacing frequencies, convergence of CV (and wavelength) occurred, with only T remaining statistically different from the other groups. Furthermore, longitudinal propagation in combination scaffolds (CL) was depressed compared to L in the presence of isotropic neighboring regions, while presence of an aligned neighbor accelerated conduction in the isotropic region (CI), so that CVL > CVCL > CVCI > CVI (similarly WL > WCL > WCI > WI). These results were measured 0.5 to 2 mm away from the anisotropic/isotropic border, a distance larger than the space constant of 360 μm.[24] Spatial mapping of calcium activation further confirmed these findings in combination samples and showed a monotonic gradient of CV across the anisotropic/isotropic border (Fig. 4C, D).

Considering the observed prolongation in APD and CTD in anisotropic samples, consistent with hypertrophic changes, we measured cell size from confocal images and quantified release of atrial natriuretic factor (ANF). Cells were significantly larger in the anisotropic samples (P < 0.01, Fig. 5A). Preliminary results on ANF as a marker of hypertrophy, also showed a significantly larger amount secreted in pure anisotropic samples compared with isotropic controls (P < 0.01, Fig. 5B).

Discussion

Hypertrophic Prolongation of APD and CTD in Anisotropy is Direction-Independent

An unexpected functional change observed in this study was the significant prolongation of APD and CTD in anisotropic structures (compared to isotropic controls) for both longitudinal and transverse propagation (Fig. 2). Based on electrotonus effects on propagation alone, one would predict AP and CT prolongation in L but not T.[25-27] Furthermore, combination scaffolds exhibited intermediate APD values between anisotropic and isotropic samples. A possible mechanism for these results is outlined in

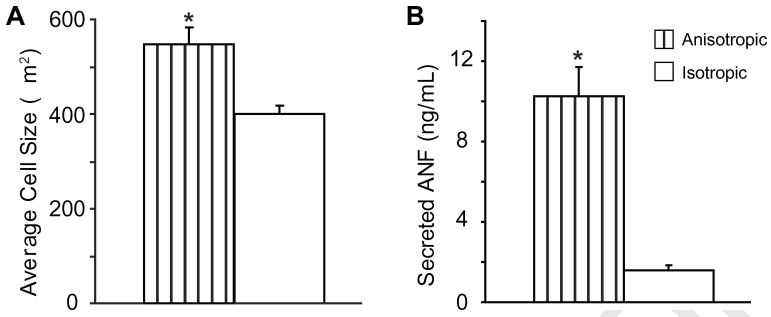

Figure 5. *Quantification of hypertrophic growth in anisotropic cultures. (A) Significantly increased cell size was seen in confocal images of the anisotropic cells as compared to isotropic controls ($P < 0.01$). (B) Quantification of ANF secreted over 24 hours showed a hypertrophy-like increase in anisotropic samples ($n = 10$) over isotropic controls ($n = 11$).*

Figure 6. As commented in Wilders *et al*., the altered loading conditions in the anisotropic networks allow easier propagation of ectopic beats.[28] Higher likelihood for "surviving" ectopic beats leads to facilitated self-sustained pacing (Fig. 7A). Indeed, in anisotropic cultures, we have confirmed higher incidence of synchronized spontaneous activity and facilitated pacemaking accompanying altered calcium dynamics.[19,29] This increased pacemaking and constant stimulation are known to lead to hypertrophy-like conditions via electrical and mechanical mechanisms.[30–32] (Fig. 6B) In our system, increased mechanical stress is due to persistent stretch of cells attached to 3D topographic features[19,20,29] and leads to significant hypertrophic growth (Fig. 5A). We have previously shown indirect evidence of hypertrophic growth, including increased strain development, higher systolic calcium, increased sarcoplasmic reticulum calcium content, upregulated connexin 43, and significantly elongated nuclei.[19,20,29] In the above-described scenario, altered mechanical loading during anisotropic growth can trigger hypertrophy-consistent prolongation of the AP and CT without the presence of external electrical or mechanical stimulation.

Our results follow several controversial findings regarding APD and cell alignment. While some studies have confirmed increase in APD along the direction of propagation due to larger electrotonus,[25,26,33] others have shown region-specific differences, for example, only in right, but not left ventricular epicardial tissue.[34] This unclear relationship between electrotonic load and APD may indicate that other modulators of APD are present in aligned cells. A well-known consequence of mechanical stress and hypertrophic growth that may play a role in determining APD is altered molecular signaling (Fig. 6B). A well-studied example is angiotensin II, which is increased in cases of pressure overload and stress-induced hypertrophy and has been shown to remodel several ionic currents, including Ito, ICaL, and IKr.[35] In addition, hypertrophic growth is accompanied by increased secretion of ANF—a rather specific and strong indicator of cardiac hypertrophy.[23] Recent studies have shown the potential of ANF to act not only as an endocrine factor regulating blood volume, but also as a local autocrine factor.[36] In our anisotropic samples, we saw increased ANF secretion (Fig. 5B), providing further evidence for hypertrophy development in conditions

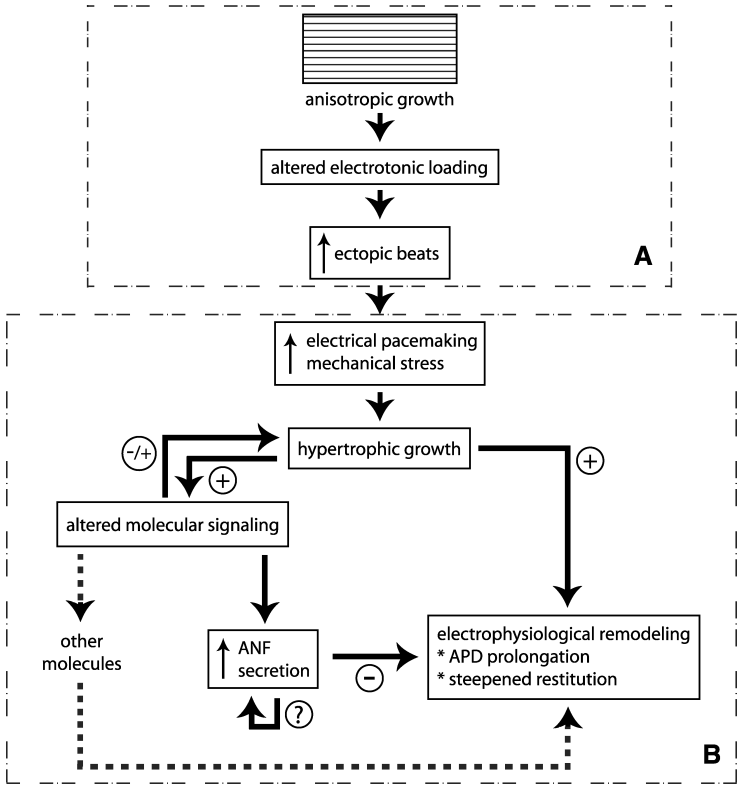

Figure 6. *Hypothesized mechanism of anisotropy-related functional differences. (A) Postulated link between anisotropic structure and increased incidence of ectopic activity due to altered electrotonic loading. (B) Established pathways of cardiac electrophysiological remodeling in response to pacing and mechanical stress show a complex interaction between molecular signaling and tissue structure.*

of anisotropic growth. By means of the ANF/cyclic GMP signaling pathway, the structural changes in hypertrophy can result in remodeling of ICaL.[36,37] While in this study no causal relationship between increased ANF and electrophysiological remodeling is confirmed, our results provide a potential mechanism for ion channel remodeling in anisotropic cell networks. Walsh *et al*. showed that elongated cell morphology increased L-type calcium channel density and protein expression.[38] Overall, modulation of structure can produce a myriad of functional changes, at least partially brought about by altered loading conditions, and potentially by changing molecular signaling (Fig. 6). By prolonging APD, the likelihood of wavefront–waveback interactions is increased and may facilitate the development of conduction blocks and arrhythmias.

Restitution is Dependent on Cell Alignment and Electrotonus

Directional dependence of restitution with greatest restitution slope of CV, APD, and wavelength in longitudinal propagation (Fig. 3) is a new finding. Restitution is brought about by the intrinsic kinetics of the ion channels; Qu *et al*. showed that APD restitution was steepened by sodium and calcium channel dynamics, while CV restitution was altered in response to sodium channel restitution kinetics.[15] Additionally, Kucera *et al*. also showed evidence of co-localization of sodium channels with gap junctions at intercalated discs.[39] Therefore, the steepened restitution in L is likely a combinatory effect from increased electrotonic load (greater number of gap junctions) and spatial redistribution of sodium channels. The dependence of restitution on the direction of wave propagation, shown here, indicates the heterogeneous nature of cardiac tissue's dynamic response. It is not immediately apparent whether the steepened APD restitution in L will promote increased development of undesirable alternans, because as shown in computational studies, the parallel steeper CV restitution and increased electrotonus via AP and CT morphology may play a counteracting stabilizing role.[17,18] The relative contribution of APD and CV restitution steepness in the promotion of instabilities deserves further attention, given the prominent modulatory role that anisotropic structure has on these parameters. This heterogeneity in functional properties (restitution) also has implications for experimental studies—restitution curves measured under different electrode configurations and wave propagation directions with respect to tissue alignment may yield varied results. We provide experimental support for the idea of quantification of restitution by histogram-based methods, as described by Fenton *et al*.,[40] so that a family of restitution relationships could be revealed and linked to structure and wave direction.

The different structural groups in this study exhibited different restitution responses, yet APD, CTD, and CV values converged at higher pacing frequencies. This is an expected outcome—as the cell networks are paced at faster frequencies ion channel kinetics becomes a limiting factor up to a conduction block. Thus, at higher frequencies, the differences brought about by electrotonic loading are minimized and ion channel dynamics become the limiting factor in cell response. Even so, the differential characteristics of the system over a range of frequencies (restitution), dictated by structure, are important in tissue adaptation to changing pacing rates.

Remote Effects of Anisotropy on Electrical Function

We used a novel method of growing tissue of different structures adjacent to each other in order to isolate the functional effects of structural remodeling found in situations similar to the border zone of myocardial infarction, for example. Our results showed a gradient of conduction velocity and wavelength across the border between networked anisotropic and isotropic regions with mutual influence between the two regions (Fig. 4A, B). In combination structures, areas of aligned cells had decreased CV, as compared with pure anisotropic growth, and isotropic areas of combination structures had increased CV, as compared with pure isotropic controls, so that overall CVL > CVCL > CVCI > CVI. This was matched also for wavelength measurements. Optical mapping revealed curvature of the wavefront across the anisotropic/isotropic border with a concave front in CI and a convex front in CL (Fig. 4C, D). Such curvature effects can act as modulators of conduction velocity by either converging (concave) or diverging (convex) excitatory currents due to the nonplanar wavefront.[1,41] Wavefront curvature effects at the border are likely to affect not only CV, but also to contribute to equalizing changes in APD in the isotropic and anisotropic portion of the scaffold,[42] as seen in our experiments.

In addition to curvature effects, remote action may also be felt via paracrine/autocrine effects. As mentioned previously, structural remodeling and alignment of cells can result in altered molecular signaling, as seen in ventricular release of ANF in hypertrophy. Indeed, preliminary results indicate increased secretion of ANF in our anisotropic samples, as compared with isotropically grown cells (Fig. 5B). In the case of combination samples, molecular signaling may be partly responsible for the dose-like response of CV and wavelength (Fig. 4A, B), in addition to loading considerations. Our results indicate that effects of remodeled structure on function can extend beyond a space constant distance by altering wave curvature and molecular signaling.

Conclusions

Our results demonstrate that anisotropic tissue growth can affect electrical function both independent and dependent of the direction of propagation and electrotonic loading. The resultant electrophysiological changes alter the electrical stability of aligned cells: (1) Lengthened APD and CTD may result in increased chance of wavefront–waveback interactions causing conduction blocks, (2) Steepened slope of APD and CV restitution may affect the induction of alternans, the precursor to fibrillation, and (3) functional consequences of locally altered structure can extend over distance by wavefront curvature-related mechanisms. We outline in Figure 6 a proposed mechanism for anisotropy-driven functional changes, linking the studies of Wilders *et al*.[28] that presented a relationship between altered electrotonus and greater ectopic activity with previously established pathways of electrophysiological remodeling in response to pacing and mechanical stress.[30–32] While structural disease can result in ion channel remodeling at the cellular level, we show that the multicellular arrangement and alignment can serve as a potent modulator of electrophysiological function. This is of particular consequence to diseased states, such as hypertrophy and myocardial infarct, in which hypertrophic anisotropic structure

initially comes about as an adaptive mechanism in order to compensate for lost contractile function. Our results indicate that such changes in structure, while mechanically optimal, may lead to compromised electrical stability. Extrapolating from our results, there is need for proper models, both *in vitro* and *in silico*, taking into account the complexity of cardiac structure and alignment in order to develop effective therapies for the problems seen in structural heart disease.

Acknowledgment: The authors would like to acknowledge Rupinder Singh, Lenny Varghese, Ujas Shah, Ravi Desai, Mohit Sharma, and Salmon Kalkhoran for assisting in experiments and culture preparations.

References

1. Wolk R, Cobbe SM, Hicks MN, Kane KA: Functional, structural, and dynamic basis of electrical heterogeneity in healthy and diseased cardiac muscle: Implications for arrhythmogenesis and anti-arrhythmic drug therapy. Pharmacol Ther 1999;84:207-231.
2. Luke RA, Saffitz JE: Remodeling of ventricular conduction pathways in healed canine infarct border zones. J Clin Invest 1991;87:1594-1602.
3. Peters NS, Green CR, Poole-Wilson PA, Severs NJ: Reduced content of connexin43 gap junctions in ventricular myocardium from hypertrophied and ischemic human hearts. Circulation 1993;88:864-875.
4. Peters NS, Wit AL: Myocardial architecture and ventricular arrhythmogenesis. Circulation 1998;97:1746-1754.
5. Weber KT, Brilla CG: Pathological hypertrophy and cardiac interstitium. Fibrosis and renin-angiotensin-aldosterone system. Circulation 1991;83:1849-1865.
6. Gaughan JP, Hefner CA, Houser SR: Electrophysiological properties of neonatal rat ventricular myocytes with alpha1-adrenergic-induced hypertrophy. Am J Physiol 1998;275:H577-H590.
7. Tomaselli GF, Marban E: Electrophysiological remodeling in hypertrophy and heart failure. Cardiovasc Res 1999;42:270-283.
8. Furukawa T, Kurokawa J: Potassium channel remodeling in cardiac hypertrophy. J Mol Cell Cardiol 2006;41:753-761.
9. Nabauer M, Kaab S: Potassium channel down-regulation in heart failure. Cardiovasc Res 1998;37:324-334.
10. Hill JA: Electrical remodeling in cardiac hypertrophy. Trends Cardiovasc Med 2003;13:316-322.
11. Kleber AG, Fast VG, Rohr S: Continuous and Discontinuous Propagation. In Zipes DP, Jalife J, editors: *Cardiac Electrophysiology: From Cell to Bedside*. Philadelphia, PA: W.B. Saunders, 2000. p. 205–213.
12. Spach MS, Heidlage JF, Dolber PC: The Dual Nature of Anisotropic Discontinuous Conduction in the Heart. In Zipes DP, Jalife J, editors: *Cardiac Electrophysiology: From Cell to Bedside*. Philadelphia, PA: W.B. Saunders , 2000. p. 213-222.
13. Henriquez CS, Muzikant AL, Smoak CK: Anisotropy, fiber curvature, and bath loading effects on activation in thin and thick cardiac tissue preparations: simulations in a three-dimensional bidomain model. J Cardiovasc Electrophysiol 1996;7:424-444.
14. Karma A: Electrical alternans and spiral wave breakup in cardiac tissue. Chaos 1994;4:461-472.
15. Qu Z, Weiss JN, Garfinkel A: Cardiac electrical restitution properties and stability of reentrant spiral waves: A simulation study. Am J Physiol 1999;276:H269-H283.
16. Tolkacheva EG, Schaeffer DG, Gauthier DJ, Krassowska W: Condition for alternans and stability of the 1:1 response pattern in a "memory" model of paced cardiac dynamics. Phys Rev E Stat Nonlin Soft Matter Phys 2003;67:031904.
17. Cytrynbaum E, Keener JP: Stability conditions for the traveling pulse: Modifying the restitution hypothesis. Chaos 2002;12:788-799.
18. Cherry EM, Fenton FH: Suppression of alternans and conduction blocks despite steep APD restitution: Electrotonic, memory, and conduction velocity restitution effects. Am J Physiol Heart Circ Physiol 2004;286:H2332-H2341.
19. Bien H, Yin L, Entcheva E: Cardiac cell networks on elastic microgrooved scaffolds. IEEE Eng Med Biol Mag 2003;22:108-112.
20. Entcheva E, Bien H: Tension development and nuclear eccentricity in topographically controlled cardiac syncytium. J Biomed Microdev 2003;5:163-168.
21. Carmeliet E: Influence of rhythm on the duration of the action potential of the heart ventricle. Arch Int Physiol Biochim 1955;63:126-127.
22. Bien H, Yin L, Entcheva E: Calcium instabilities in mammalian cardiomyocyte networks. Biophys J 2006;90:2628-2640.
23. Swynghedauw B: Molecular mechanisms of myocardial remodeling. Physiol Rev 1999;79:215-262.
24. Jongsma HJ, van Rijn HE: Electronic spread of current in monolayer cultures of neonatal rat heart cells. J Membr Biol 1972;9:341-360.
25. Bursac N, Parker KK, Iravanian S, Tung L: Cardiomyocyte cultures with controlled macroscopic anisotropy: a model for functional electrophysiological studies of cardiac muscle. Circ Res 2002;91:e45–e54.
26. Gotoh M, Uchida T, Fan W, Fishbein MC, Karagueuzian HS, Chen PS: Anisotropic repolarization in ventricular tissue. Am J Physiol 1997;272:H107-H113.
27. Zubair I, Pollard AE, Spitzer KW, Burgess MJ: Effects of activation sequence on the spatial distribution of repolarization properties. J Electrocardiol 1994;27:115-127.
28. Wilders R, Wagner MB, Golod DA, Kumar R, Wang YG, Goolsby WN, Joyner RW, Jongsma HJ: Effects of anisotropy on the development of cardiac arrhythmias associated with focal activity. Pflugers Arch 2000;441:301-312.
29. Yin L, Bien H, Entcheva E: Scaffold topography alters intracellular calcium dynamics in cultured cardiomyocyte networks. Am J Physiol Heart Circ Physiol 2004;287:H1276-H1285.
30. Kira Y, Nakaoka T, Hashimoto E, Okabe F, Asano S, Sekine I: Effect of long-term cyclic mechanical load on protein synthesis and morphological changes in cultured myocardial cells from neonatal rat. Cardiovasc Drugs Ther 1994;8:251-262.
31. Sadoshima J, Izumo S: The cellular and molecular response of cardiac myocytes to mechanical stress. Annu Rev Physiol 1997;59:551-571.
32. McDonough PM, Glembotski CC: Induction of atrial natriuretic factor and myosin light chain-2 gene expression in cultured ventricular myocytes by electrical stimulation of contraction. J Biol Chem 1992;267:11665-11668.
33. Osaka T, Kodama I, Tsuboi N, Toyama J, Yamada K: Effects of activation sequence and anisotropic cellular geometry on the repolarization phase of action potential of dog ventricular muscles. Circulation 1987;76:226-236.
34. Bertran G, Biagetti MO, Valverde E, Arini PD, Quinteiro RA: Lack of effect of conduction direction on action potential durations in anisotropic ventricular strips of pig heart. J Cardiovasc Electrophysiol 2002;13:380-387.
35. Rosen MR, Cohen IS: Cardiac memory . . . new insights into molecular mechanisms. J Physiol 2006;570:209-218.
36. Nishikimi T, Maeda N, Matsuoka H: The role of natriuretic peptides in cardioprotection. Cardiovasc Res 2006;69:318-328.
37. Tokudome T, Horio T, Kishimoto I, Soeki T, Mori K, Kawano Y, Kohno M, Garbers DL, Nakao K, Kangawa K: Calcineurin-nuclear factor of activated T cells pathway-dependent cardiac remodeling in mice deficient in guanylyl cyclase A, a receptor for atrial and brain natriuretic peptides. Circulation 2005;111:3095-3104.
38. Walsh KB, Parks GE: Changes in cardiac myocyte morphology alter the properties of voltage-gated ion channels. Cardiovasc Res 2002;55:64-75.
39. Kucera JP, Rohr S, Rudy Y: Localization of sodium channels in intercalated disks modulates cardiac conduction. Circ Res 2002;91:1176-1182.
40. Fenton FH, Cherry EM, Hastings HM, Evans SJ: Multiple mechanisms of spiral wave breakup in a model of cardiac electrical activity. Chaos 2002;12:852-892.
41. Fast VG, Kleber AG: Role of wavefront curvature in propagation of cardiac impulse. Cardiovasc Res 1997;33:258-271.
42. Qu Z, Xie F, Garfinkel A, Weiss JN: Origins of spiral wave meander and breakup in a two-dimensional cardiac tissue model. Ann Biomed Eng 2000;28:755-771.

Query

Q1 Author: Please provide figure 7 with caption .